ACS OMEGA

Open Access

http://pubs.acs.org/journal/acsodf

Article

Distal Domains of the Bacterial-Exclusive Wobble-Modifying Enzyme TilS Contribute to Catalysis

Ferdiemar C. Guinto, Jr., Samantha C. Robinson, and Rebecca W. Alexander*

Cite This: *ACS Omega* 2025, 10, 11618−11626

Read Online

ACCESS | Metrics & More | Article Recommendations | Supporting Information

ABSTRACT: $tRNA^{Ile2}$ lysidine synthetase (TilS) is a bacterial-specific wobble-modifying enzyme that acts on the isoleucine-accepting $tRNA^{Ile2}_{CAU}$. TilS installs a lysine at the C34 position of the anticodon, generating the lysidine modification. The resulting LAU anticodon enables exclusive decoding of infrequently used AUA isoleucine codons, rejecting AUG methionine codons. Compared to other wobble-modifying enzymes that contact only the anticodon arm of their cognate tRNAs, TilS is distinct in containing additional domains outside of the N-terminal active site. For type I TilS enzymes such as the *B. cenocepacia* TilS (BcTilS) investigated here, appended domains contact the $tRNA^{Ile2}$ substrate along the body and through the acceptor stem, up to 60 Å away from the target C34. Among bacterial tRNAs, only unmodified $tRNA^{Ile2}$ and $tRNA^{Met}$ share an anticodon, suggesting that the appended domains of TilS provide substrate recognition strategies that other wobble-modifying enzymes do not need. Here, we investigate both protein and tRNA elements to understand the strategy by which TilS accepts its cognate $tRNA^{Ile2}$ substrate and rejects the near-cognate $tRNA^{Met}$.

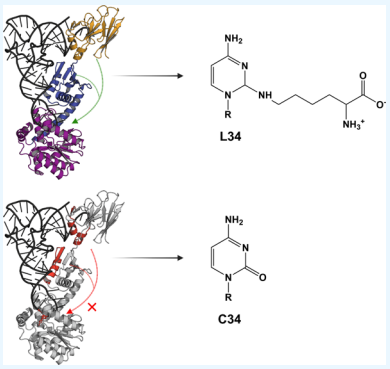

INTRODUCTION

Post-transcriptional modification expands the chemical and structural properties of RNA beyond the four encoded ribonucleotides.[1−3] tRNAs are the most densely decorated class of RNAs, with over 100 distinct modifications identified to date; each mature bacterial tRNA contains 7−8 modified positions among their ∼ 76 nucleotides.[3,4] Such modifications contribute to the folding and structure of tRNA (especially in the tRNA body) or affect translation by altering the decoding capabilities of the tRNA (when located in or adjacent to the anticodon).[1] Wobble modifying enzymes act on the N34 position to ensure accurate decoding at the ribosome.[5] Some wobble modifications expand decoding rules, such as deamination of A34 to inosine, which enables a single tRNA isoacceptor to decode three mRNA codons.[6,7] Other modifications at N34 fine-tune the codon-anticodon structure in the ribosomal A-site. This may be best exemplified by mnm^5s^2U34, which acts on $tRNA^{Glu}$ and $tRNA^{Lys}$, changing translation rates for the codons recognized by these tRNAs.[8]

The lysidine wobble modification that is installed in bacterial $tRNA^{Ile2}$ goes beyond expanding or restricting decoding, in that it switches anticodon specificity.[9−13] Three codons correspond to isoleucine in the standard genetic code: AUA, AUC, and AUU. Of these, AUA is typically used at lower frequency than the other two and requires adaptation of the translational machinery.[14] Standard Watson−Crick pairing rules dictate that the isoleucine AUA codon should be decoded by a UAU-containing anticodon. However, because of wobble pairing, a $tRNA_{UAU}$ could decode both AUA (isoleucine) and AUG (methionine) codons, resulting in isoleucine misincorporation at methionine positions. The bacterial-specific tRNA isoleucine lysidine synthetase (TilS) modifies the C34 wobble position of the minor acceptor $tRNA^{Ile2}_{CAU}$ by installing a lysine moiety at this position, generating the modified base lysidine (L34).[9−13] Mature $tRNA^{Ile2}_{LAU}$ rejects the AUG codon and decodes AUA exclusively.[15,16] Plant organelles and some bacteria were recently determined to contain 2-aminovaleramididine (ava^2C) at the $tRNA^{Ile2}$ wobble position; ava^2C likely derives from L, although the enzyme responsible has not yet been identified.[17] Archaea solve the AUA challenge in a similar way, where TiaS modifies the C34 wobble position to agmatidine (agm^2C).[18−22] Lysidine, ava^2C, and agm^2C all promote AUA decoding at the ribosome using a similar pattern of hydrogen bonding, such that a single H-bond to the wobble adenine is supplemented by an additional H-bond between the extended C34 modification and the 2′−OH of the base following the AUA codon.[16,17,23] Some bacteria (such as *Mycoplasma mobile*) lack the tilS gene, and both isoleucyl-tRNA synthetase and the ribosomal machinery have evolved to differentiate between AUA and AUG codons using $tRNA^{Ile2}_{UAU}$.[24] Eukaryotes

Received: January 29, 2025
Revised: February 23, 2025
Accepted: March 7, 2025
Published: March 14, 2025

modify the wobble position of $tRNA^{Ile2}_{UAU}$ to pseudouridine to ensure aminoacylation and decoding specificity.[25]

There are six well-characterized wobble modifying enzymes in bacteria, of which four have solved crystal structures.[26] While other wobble modifying enzymes are small and contact just the anticodon, TilS enzymes have at least one domain outside the active site that reaches to the anticodon stem and the elbow of the L-shaped tRNA.[27−31] About one-third of TilS enzymes contain a single appended domain C-terminal to the catalytic core (CTD1); these enzymes are Type II TilS homologues. Most TilS homologues (Type I enzymes) have both the CTD1 and a second C-terminal domain (CTD2) that contacts the acceptor stem ∼ 60 Å from the active site. If the purpose of these appended protein modules is to enhance substrate specificity, there may be a difference in how the two classes of TilS identify their cognate substrate and reject near-cognate tRNAs.

Our prior selection experiments revealed strains of *Burkholderia cenocepacia* with mutations in *tilS* that evolved in response to nutrient deficient growth by emerging from lag-phase growth faster than the ancestral strain.[32] Biochemical analysis of these TilS variants revealed that each enzyme displayed a notable decrease in lysidinylation activity. Further, each mutation was remote from the catalytically active N-terminal domain (NTD), ranging ∼ 30−70 Å away from the active site in the CTD1 and CTD2 domains.[32] To better understand the phenotype of these evolved mutations, we set out to investigate the substrate selection strategies of BcTilS. We hypothesize that nucleotides in the acceptor stem and the anticodon stem are recognized by amino acids in CTD2 and CTD1, respectively, promoting efficient enzyme activity. Here we use the BcTilS system to explore atomic-level interactions that contribute to catalysis at a distance.

MATERIALS AND METHODS

Enzyme Cloning and Mutagenesis. The *B. cenocepacia tilS* gene (UniProt ID A0A3R9CE37) was isolated from chromosomal DNA and cloned into a pET-28a expression vector (Invitrogen) as previously described.[32] Enzyme variants were achieved through site-directed mutagenesis using standard QuikChange strategies.[33−35] Substitutions were made in BcTilS using the *Geobacillus kaustophilus* TilS (GkTilS) structure in complex with *B. subtilis* $tRNA^{Ile2}$ (PDB 3A2K)[29] and a Clustal Omega alignment of TilS homologues.[36] BcTilS is 19.6% identical and 40.2% similar to GkTilS, as determined using the online Sequence Manipulation Suite tool.[37] Primer sequences are available on request. Mutations were confirmed by Sanger sequencing (Azenta Life Sciences, azenta.com).

Protein Expression and Purification. Protein expression and purification were carried out as described.[32] Sequence-verified plasmids were transformed into *E. coli* Top 10 competent cells for storage and *E. coli* Rosetta II (DE3) (Invitrogen) expression strain for protein expression. Individual transformant colonies were isolated and starter inoculant cultures were grown in LB with 35 μg/mL kanamycin for 16−18 h at 37 °C. Starter inoculants were added to LB/Kan expression cultures and grown at 37 °C shaking at ∼ 200 rpm for roughly 2−5 h. Once OD_{600} measured between 0.4 and 0.6, induction was achieved by the addition of isopropyl β-D-1-thiogalactopyranoside (IPTG) to 1 mM. Expression proceeded for 2−6 h and cells were harvested and either stored at −20 °C or immediately purified. For purification, pelleted cells were resuspended in buffer A (20 mM Tris-HCl [pH 8.0], 150 mM NaCl, 20 mM imidazole), subjected to lysis by sonication (15% amplitude for 5 min at intervals of 5 s on and 5 s off), and soluble fractions were passed over Ni^{2+} columns using a BioRad DuoFlow FPLC. Each protein of interest was eluted with high imidazole content buffer B (20 mM Tris-HCl [pH 8.0], 150 mM NaCl, 500 mM imidazole) with fractions dialyzed against storage buffer (40 mM Tris-HCl [pH 8.0], 200 mM NaCl, 20 mM $MgCl_2$, 20 mM KCl, 40% glycerol). Isolated proteins were analyzed by 10% SDS-PAGE to confirm size and heterogeneity. Protein concentrations were determined by UV absorbance (ThermoScientific, Nanodrop 2000c spectrophotometry) and Bio-Rad Bradford protein assay and stored at −20 °C.

***In Vitro* tRNA Synthesis.** *In vitro* tRNA synthesis was performed as described.[32,38] Briefly, overlapping oligonucleotide primers were used to synthesize double stranded DNA templates for subsequent RNA synthesis reactions. Primers were designed based on sequences found in the Genomic tRNA database (GtRNADB) (http://gtrnadb.ucsc.edu/).[39,40] Primer sequences are available on request. Reactions consisted of 4 μM of each tRNA primer, 1 mM dNTP mix, 10x NEB 2 Buffer (New England Biolabs Inc.), and 10 μL/mL Klenow enzyme (New England Biolabs Inc.). Duplex DNA products were used as templates for T7 RNA polymerase reactions. Transcription reactions were incubated overnight at 37 °C in 200 mM Tris-HCl (pH 7.5), 30 mM $MgCl_2$, 0.1 mg/mL Bovine serum albumin (BSA), 2 mM spermidine, 40 mM dithiothreitol, 5 mM of each NTP, and T7 RNA polymerase (purified in house). Products were recovered by ethanol precipitation and purified by gel electrophoresis on 8 M urea/10% acrylamide SDS-PAGE gels. The final tRNA product was eluted from the gel fragments with 500 mM ammonium acetate elution buffer (pH 5.3) and recovered by ethanol precipitation. The resulting tRNA was resuspended in TE buffer, quantified by UV absorbance (ThermoScientific, Nanodrop 2000c spectrophotometry), and stored at −20 °C.

Lysidinylation Assay. A filter-pad binding assay was used to monitor the catalytic activity of TilS. $tRNA^{Ile2}$ was annealed by heating at 80 °C for 5 min in 10 mM TE buffer, followed by cooling to 65 °C at which point $MgCl_2$ was added (final concentration 10 mM) to aid in folding. Reactions contained 100 mM Tris-HCl (pH 9.0), 5 mM DTT, 10 mM $MgCl_2$, 10 mM KCl, and 2 mM ATP. ^{3}H-lysine was added to the reaction mix followed by tRNA (final concentration 2 μM). The total concentration of lysine was 14.75 μM, of which 5 μM was unlabeled L-lysine and 9.75 μM was [4,5-^{3}H(N)]L-lysine (Moravek Inc., La Brea, CA). Reactions were initiated by the addition of TilS (final concentration 500 nM unless otherwise indicated). Reaction aliquots (5 μL) were quenched on presoaked Whatman filter pads containing 5% TCA. After time points were taken, accumulated quench pads were washed four times for 10 min each in 200−300 mL 5% TCA to remove unreacted ^{3}H-lysine. Filter pads were subsequently dried, placed in vials containing 4 mL of scintillation fluid, allowed to equilibrate for 20 min, then evaluated by scintillation counting.

Data Analysis. Total radioactive signal was determined from scintillation data. Counts present in the negative control allow the attribution of signal to total lysine (3H-labeled + unlabeled) in the reaction, while negative control washes allow the subtraction of background. Each time point was transformed into pmols of lysidine product formed, and initial rates were determined from the linear portion of the progress curve (GraphPad Prism). Relative rates were determined for each

https://doi.org/10.1021/acsomega.5c00897
ACS Omega 2025, 10, 11618−11626

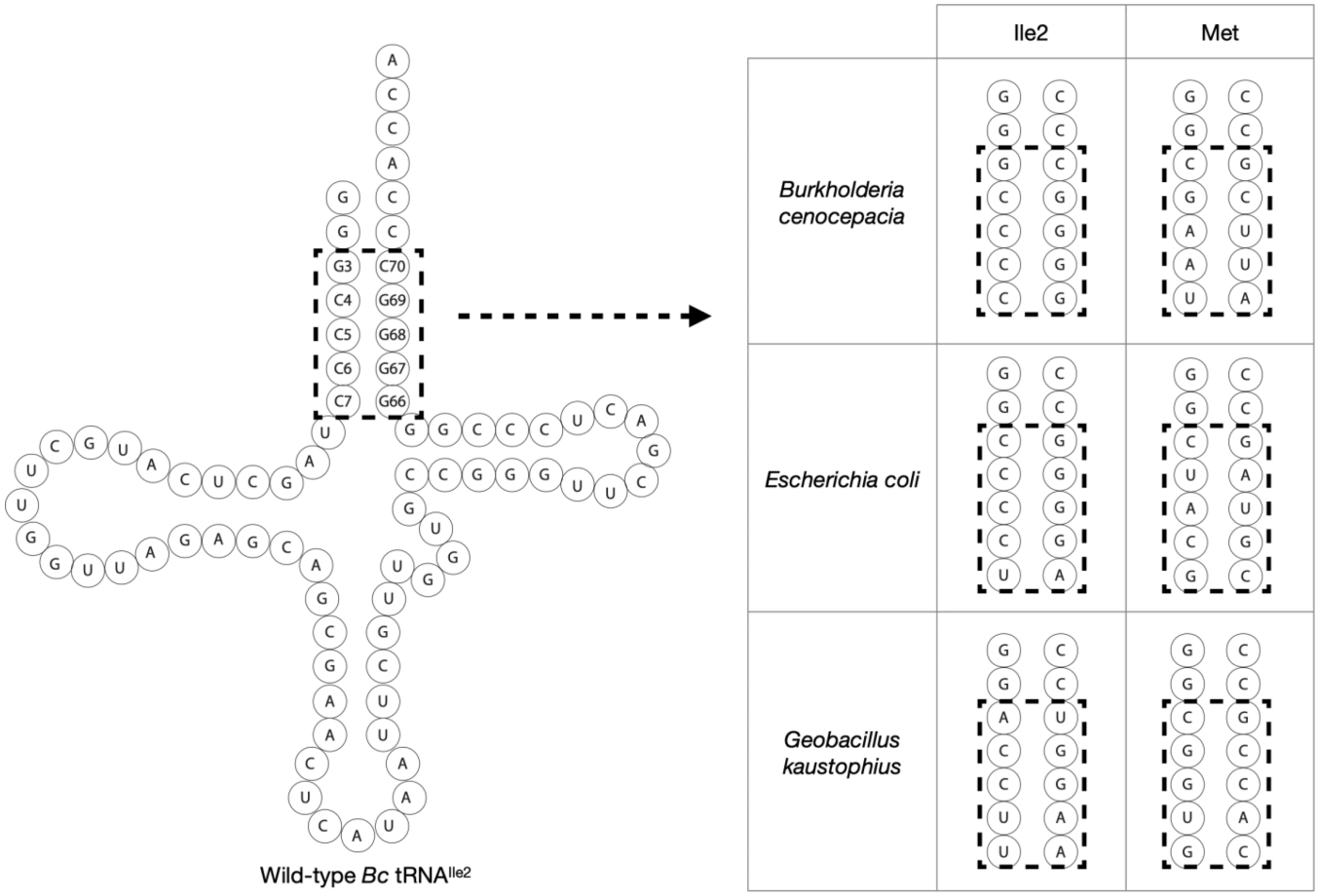

Figure 1. Acceptor stem sequences of $tRNA^{Ile2}$ provide discrimination against noncognate $tRNA^{Met}_{CAU}$. Left: The full sequence/clover leaf representation for wild-type *B. cenocepacia* $tRNA^{Ile2}$. Right: Acceptor stem comparison between cognate $tRNA^{Ile2}$ and near-cognate $tRNA^{Met}$ for the three model systems.

enzyme or tRNA variant compared to the wild-type enzyme or tRNA. At least three technical replicates of each reaction were performed (unless otherwise noted), with standard deviation reported.

RESULTS

Establishing BcTilS Identity Elements in the $tRNA^{Ile2}$ Acceptor Stem. The *tilS* gene is considered essential in bacteria.[41−43] It is present in nearly all bacterial genomes and attempts to knock it out have proven lethal in the model systems *E. coli* and *B. subtilis*.[44−47] Such essentiality is presumed necessary for accurate translation of AUA codons, as the CAU anticodon of unmodified $tRNA^{Ile2}$ is not able to decode AUA. Given that $tRNA^{Met}$ also contains a CAU anticodon, nucleotides outside the anticodon must serve to select $tRNA^{Ile2}$ and reject $tRNA^{Met}$ (Figure 1). Indeed, prior work with *Escherichia coli* TilS (EcTilS) demonstrated that nucleotides in the $tRNA^{Ile2}$ acceptor stem are critical for lysidinylation activity, and the *G. kaustophilus* TilS:tRNA cocrystal structure reveals proximity between TilS and the tRNA acceptor stem.[11,29,32] To better understand the structural features of BcTilS that contribute to catalysis, we first sought to determine identity elements in *B. cenocepacia* $tRNA^{Ile2}$ ($BctRNA^{Ile2}$). Using established tRNA synthesis protocols, we produced wild-type $BctRNA^{Ile2}$ and a library of acceptor stem variants for *in vitro* lysidinylation assays.

As expected from prior characterization of the *E. coli* TilS:$tRNA^{Ile2}$ system, nucleotides in the $BctRNA^{Ile2}$ acceptor stem contribute significantly to BcTilS catalysis. We observed that the 3:70 and 4:69 base pairs are most critical, as inversions at these positions (G3:C70 → C3:G70 and C4:G69 → G4:C69) nearly abolish enzymatic activity (Figure 2, Table S1). In contrast, base pairs further down the acceptor stem do not contribute substantially to substrate recognition, with base inversions at the 5:68, 6:67, and 7:66 positions resulting in robust catalysis. The use of 3:70 and 4:69 differs from EcTilS, which instead relies on base pairs 4:69 and 5:68 for lysidinylation identity.[11]

Given the observed importance of the 3:70 base-pair for BcTilS and the known use of this position for recognition by several aminoacyl-tRNA synthetases,[48,49] we made additional substitutions to determine if any other nucleotides can be tolerated at this position. We noted that BcTilS does not tolerate 3:70 base pair changes, as most variants result in a < 15% relative activity (Figure 2). Surprisingly, the C3:C70 substitution yielded moderate activity (~45%), suggesting that C70 may be the critical base for recognition. Alternatively, structural distortion from this noncanonical base pair may promote catalysis without direct readout of the C70 base.

A C-Terminal Helix-Turn-Helix Motif Reads Out Key Acceptor Stem Base Pairs. Having clarified which base pairs in the acceptor stem contribute most to TilS catalysis, we sought to identify key amino acids distal to the active site that

https://doi.org/10.1021/acsomega.5c00897
ACS Omega 2025, 10, 11618−11626

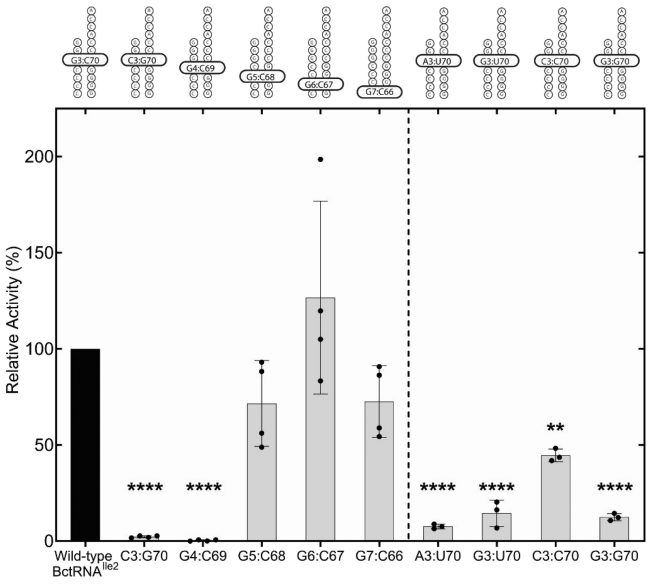

Figure 2. Two base pairs of the tRNA^{Ile2} acceptor stem are BcTilS identity elements. tRNA variants were synthesized and used in TilS lysidinylation reactions. Reactions contained 2 μM tRNA and 500 nM wild-type BcTilS. Error bars for tRNA variants are the standard deviation of 3−4 independent experiments (individual N values are reported in Table S1). *Indicates statistical significance by One-Way Anova analysis using GraphPad Prism. Unmarked indicates no significance; ** = p-value <0.01 and **** = p-value <0.0001.

might influence substrate specificity. Inspection of the *G. kaustophilus* TilS:tRNA^{Ile2} cocrystal structure (PDB 3A2K) suggested that a helix-turn-helix (HTH) motif within CTD2 could provide acceptor stem recognition.[29] This motif is comprised of a short helix (helix 1) and turn before a second helix (helix 2) with a conserved PxxxRxxxP sequence motif. The arginine in helix 2 has been established as a residue critical for EcTilS (Muraski, manuscript in preparation) and GkTilS activity[29] and is conserved across ∼ 90% of type I TilS enzymes (as evaluated by ConSurf-DB using the GkTilS to query).[50] We hypothesized that helix 1 side chains participate in direct readout of the acceptor stem major groove, while the helix 2 conserved arginine contributes electrostatic stabilization of the phosphate backbone. We subjected this HTH motif to alanine scanning, allowing us to identify residues distal to the TilS active site that influence catalysis.

Of the 12 variants, seven displayed only nominal changes to enzymatic activity (Figure 3A, Table S2). The remaining five variants exhibited notable activity loss, suggesting that residues R409, N413, Q416, P421, and R425 participate in recognition of the BctRNA^{Ile2} acceptor stem. Residues P421 and R425 are particularly noteworthy. Arginine-425 is highly conserved and contributes to catalysis in other orthologs, as noted above.[29] Proline-421 was one of four positions where BcTilS mutations evolved under nutrient-depleted conditions; a single nucleotide polymorphism resulting in a P421L mutant promoted bacterial fitness despite decreased *in vitro* and *in vivo* lysidinylation activity.[32]

With the identification of these CTD2 residues contributing to catalysis, we explored the atomic features that could be introduced at those positions to restore TilS activity. To probe the chemical importance of R409, N413, Q416, and R425, substitutions other than alanine were generated. We considered both chemical similarity to the residue in wild-type BcTilS and side chains present at corresponding locations in EcTilS and GkTilS orthologs, generating R409K, T410K, N413E, N413K, N413Q, Q416N, and R425K BcTilS variants. Overall, these changes were not tolerated, but variants R409K,

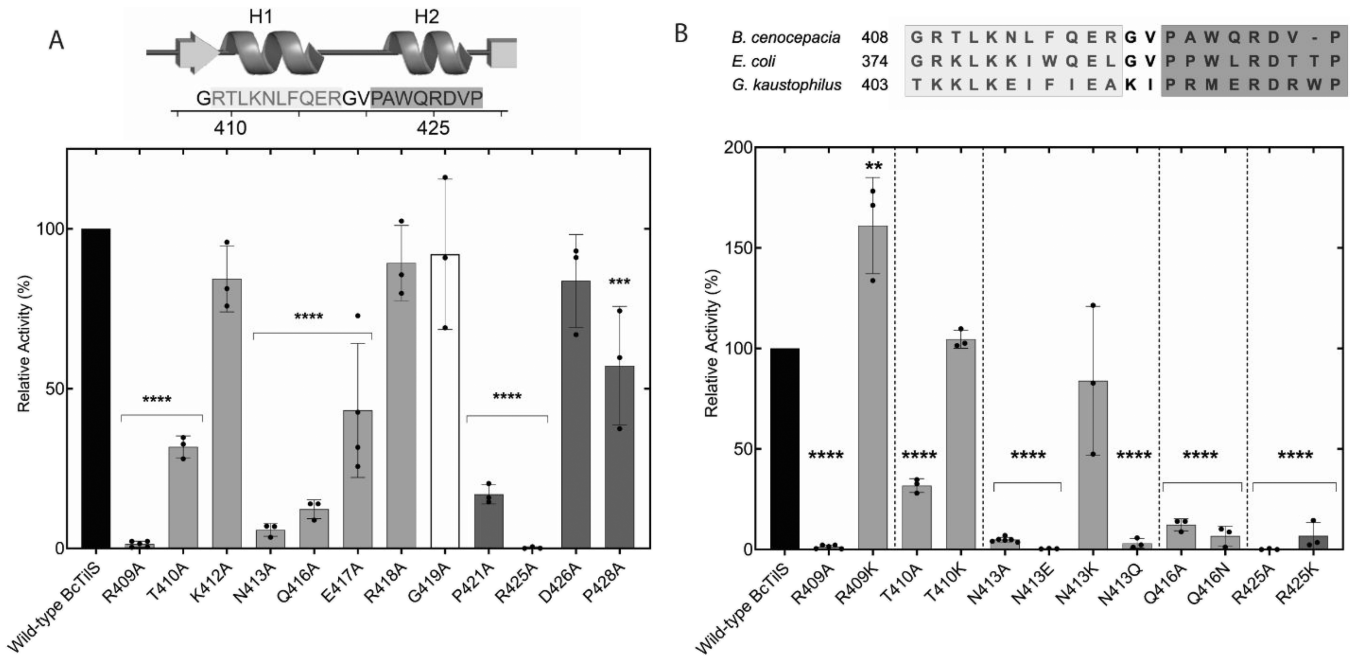

Figure 3. Residues in the CTD2 helix-turn-helix motif contribute to catalysis. A. Relative activities of HTH alanine variants compared to wild-type BcTilS. B. Sequence alignment of three TilS orthologs of interest (BcTilS, EcTilS, and GkTilS) informed selection of substitutions in the HTH, with relative activities compared to wild-type BcTilS indicated. Error bars for TilS variants are the standard deviation of 3−6 independent experiments (individual N values are reported in Table S2). *Indicates statistical significance by One-Way Anova analysis using GraphPad Prism. Unmarked indicates no significance; ** = p-value <0.01, *** = p-value <0.001, and **** = p-value <0.0001.

https://doi.org/10.1021/acsomega.5c00897
ACS Omega 2025, 10, 11618−11626

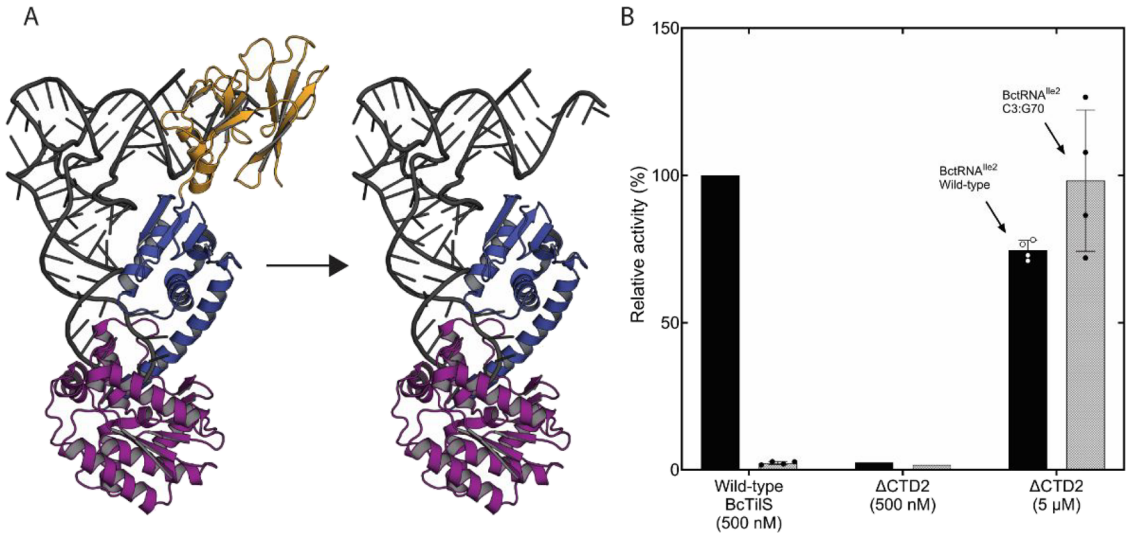

Figure 4. BcTilS ΔCTD2 variant retains activity and expands substrate use. A. Cartoon model of a truncated Type I TilS enzyme. B. Comparison of truncated enzyme to wild-type BcTilS. Wild-type $tRNA^{Ile2}$ and C3:G70 $tRNA^{Ile2}$ (2 μM) were used to determine substrate discrimination. Reactions contained 500 nM or 5 μM enzyme, as indicated. Error bars for tRNA and TilS variants are the standard deviation of four independent experiments, except for the ΔCTD2 variant which was a single preliminary assay (individual N values are reported in Table S4).

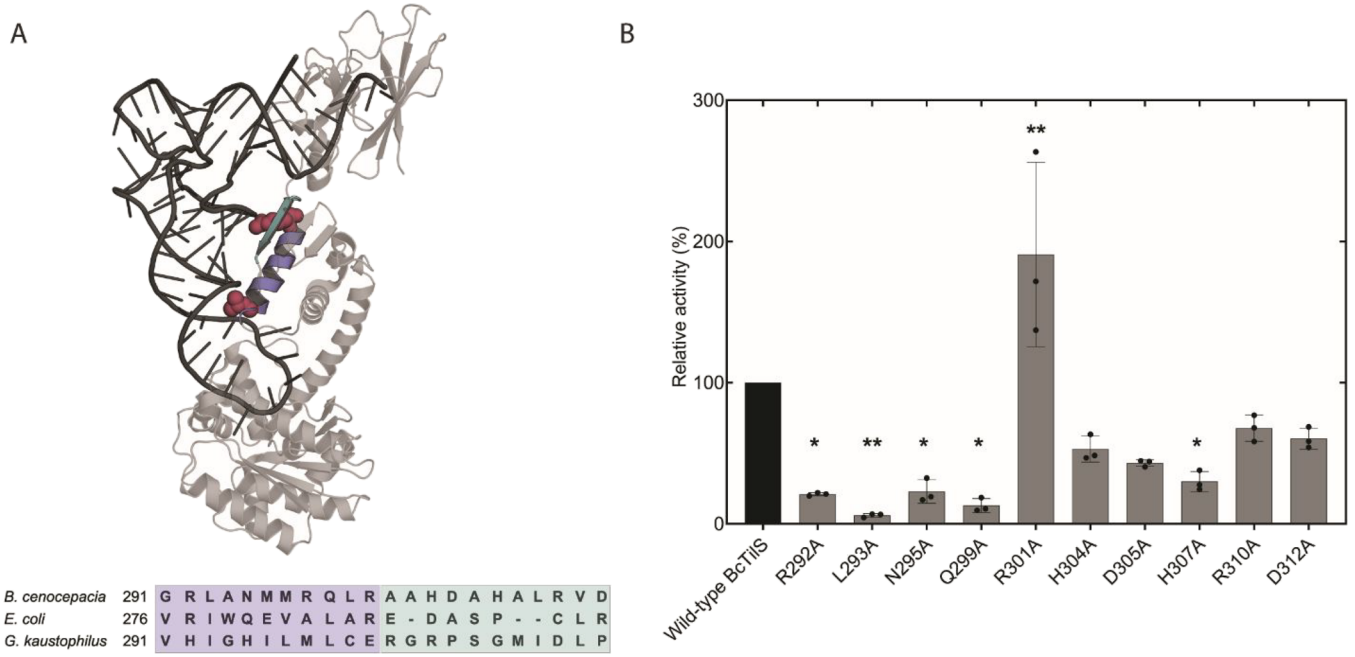

Figure 5. A CTD1 helix-turn-strand motif may read out the anticodon stem. A. The CTD1 helix-turn-strand motif is proximal to the $tRNA^{Ile2}$ anticodon stem (GkTilS:$BstRNA^{Ile2}$ structure, PDB3A2K).[29] Positions of interest are highlighted on the sequence alignment with helix residues blue and strand residues teal; residues shown in space-filling mode are GkTilS H292 and R302 (BcTilS R292 and R301). B. Relative activities of alanine variants are compared to wild-type BcTilS. Reactions contained 2 μM tRNA and 500 nM enzyme. Error bars for TilS variants are the standard deviation of three independent experiments (individual N values are reported in Table S3). *Indicates statistical significance by One-Way Anova analysis using GraphPad Prism. Unmarked indicates no significance; * = p-value <0.05, ** = p-value <0.01.

T410K, and N413K in helix 1 all restored BcTilS activity (Figure 3B, Table S2).

Deleting CTD2 Decreases TilS Activity and Removes 3:70 Discrimination. With at least five residues distal to the TilS active site affecting catalysis, we became intrigued at the role of CTD2, given that type II TilS enzymes support cellular function despite absence of this domain. We therefore generated a Type II-like BcTilS enzyme by inserting a stop codon into the loop linking the CTD1 and CTD2; this P335X variant we denoted as BcTilS ΔCTD2.

The ΔCTD2 variant is not efficient at modifying the $tRNA^{Ile2}$ substrate under typical conditions but does retain activity at elevated concentration. Furthermore, removal of CTD2 relieves acceptor stem discrimination, as the C3:G70 $tRNA^{Ile2}$ variant was an efficient substrate for the truncated enzyme (Figure 4, Table S4).

A Helix-Turn-Strand Motif in CTD1 Contributes to TilS Activity. Just as the CTD2 module promotes acceptor stem recognition, we reasoned based on structure that the CTD1 should recognize features of the $tRNA^{Ile2}$ anticodon

https://doi.org/10.1021/acsomega.5c00897
ACS Omega 2025, 10, 11618−11626

stem (Figure 5A). Anticodon stem discrimination alone is presumed sufficient for Type II enzymes, which must reject noncognate tRNAs without contacting the acceptor stem, and substitutions to the anticodon stem impair lysidinylation by Type I EcTilS.[11] We noted a helix in the CTD1 (in a helix-turn-strand motif) of the GkTilS cocrystal structure in apparent proximity to the $tRNA^{Ile2}$ anticodon stem. Residues of this motif were subjected to alanine scanning mutagenesis to determine which positions influenced TilS activity.

Unlike for CTD2, several of the CTD1 variants exhibited decreased lysidinylation, with relative activities ranging from 7 to 70% of wild-type BcTilS (Figure 5B, Table S3). Residues on the helix (R292, L293, N295, and Q299) have a greater effect, while those on the strand (H304, D305, H307, R310, and D312) are less detrimental. Surprisingly, variant R301A was able to modify $tRNA^{Ile2}$ even better than the wild-type enzyme. This may suggest that R301 is an antideterminant for noncognate tRNAs, limiting dynamic rearrangement in the absence of cognate identity elements, and removal of the side chain enables the complex to more readily access an active conformation.

The CTD1 Does Not Influence Acceptor Stem Discrimination. Substitutions in the CTD1 domain are unlikely to impact acceptor stem discrimination, given the separation of at least 25 Å. We tested this by providing the hyperactive BcTilS R301A enzyme with C3:G70 $BctRNA^{Ile2}$ (not a substrate for wild-type BcTilS, but lysidinylated by the ΔCTD2 variant). This tRNA was not a suitable substrate for the CTD1 variant R301A, even though the enzyme displayed an increased activity with wild-type $tRNA^{Ile2}$, indicating acceptor stem discrimination to be conserved in this variant (Figure 6, Table S4). We also tested $BctRNA^{Met}$ as a substrate for the ΔCTD2 and R301A enzymes. Neither the Type II TilS-like ΔCTD2 nor the BcTilS R301A variant was able to lysidinylate noncognate $tRNA^{Met}$ efficiently, even at increased concentrations, indicating that acceptor stem discrimination is not the sole mechanism for noncognate tRNA rejection.

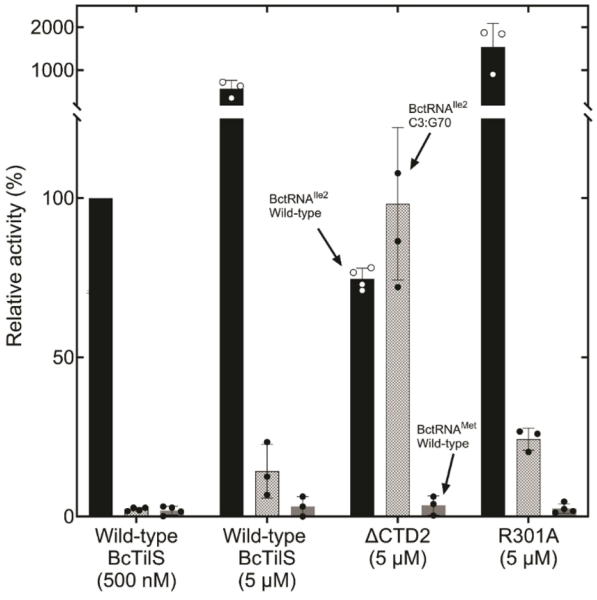

Figure 6. ΔCTD2 but not CTD1 R301A variant expands substrate recognition. The hyperactive R301A variant retains discrimination against C3:G70 $tRNA^{Ile2}$ and $tRNA^{Met}$. Enzymes were used at 500 nM or 5 μM as indicated. Error bars for tRNA and TilS variants are the standard deviation of 3−4 independent experiments (individual N values are reported in Table S4).

Combined CTD1 and CTD2 Substitutions Expand Substrate Acceptance. Finally, we sought to generate a full-length BcTilS variant that could efficiently modify a non-substrate tRNA. We reasoned that combining changes in CTD1 and CTD2 motifs proximal to the anticodon and acceptor stems, respectively, would achieve this effect. We chose the T410K substitution for the CTD2 position, as it is one of residues in the helix-turn-helix motif that varies between BcTilS with EcTilS. Indeed, combining the hyperactive CTD1 R301A variant with the robust CTD2 T410K variant generated an enzyme that could modify C3:G70 $BctRNA^{Ile}$ to ∼ 67% relative activity (Figure 7, Table S5). The enhanced lysidinylation activity was more than simply additive (the single variants achieved only 17% and 5% activity), suggesting dynamic communication between the two protein loci. Interestingly, the T410 K/R301A variant was notably more active than the wild-type BcTilS with its cognate $tRNA^{Ile2}$ as well, reaching over 350% of the wild-type enzyme activity.

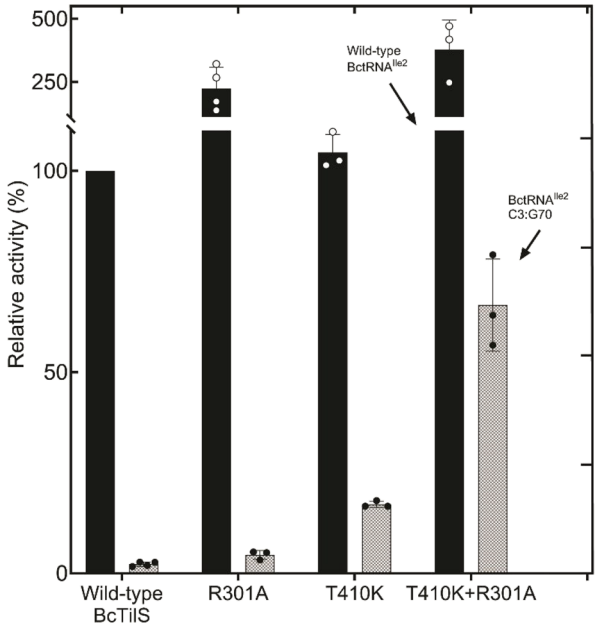

Figure 7. Substitutions in both the CTD1 and CTD2 produce a relaxed specificity enzyme. The near-cognate C3:G70 $BctRNA^{Ile2}$ is lysidinylated more efficiently by the double mutant T410K/R301A than either variant alone. Reactions contained 2 mM $tRNA^{Ile2}$ and 500 nM TilS. Error bars for tRNA and TilS variants are the standard deviation of 3−4 independent experiments (individual N values are reported in Table S5).

DISCUSSION

The bacterial-exclusive tRNA modifying enzyme TilS provides us with a useful system to probe protein-RNA recognition strategies. We anticipate that the TilS:$tRNA^{Ile2}$ pair was a late addition to the translational machinery, with TilS arising late and coevolving with its tRNA substrate after the MetRS:$tRNA^{Met}$ pair were fixed. With a rare need to differentiate between two tRNAs containing the same anticodon (a situation not observed outside of the AUN codon box), the need for specificity is critical.

https://doi.org/10.1021/acsomega.5c00897
ACS Omega 2025, 10, 11618−11626

Despite the high conservation of TilS in bacteria to ensure translation of the AUA codon, homologues vary in their domain organization, catalytic properties, and recognition strategies. While the majority exist as Type I enzymes, which range from 450 to 500 amino acids and have two C-terminal domains outside the catalytic site, others are Type II orthologs that lack CTD2, and some are even present as fusion proteins exceeding 600 amino acids.[28,51,52]

Comparing the *B. cenocepacia* enzyme with its *E. coli* counterpart, we previously observed that EcTilS exhibits a catalytic efficiency 1000-fold higher than BcTilS (Muraski, manuscript in preparation). These two enzymes also use different positions within the acceptor stem for discrimination: EcTilS uses the 4:69 and 5:68 positions as major identity elements,[11] while BcTilS instead depends on the 3:70 and 4:69 base pairs (Figure 2). This is a subtle difference, but if we examine $tRNA^{Met}$ from the respective organisms, we notice that $EctRNA^{Met}$ shares a C3:G70 base pair with $EctRNA^{Ile2}$, rendering this an unsuitable identity element for EcTilS. The *B. cenocepacia* tRNAs, in contrast, differ at the 3:70 position (Figure 1).

We sought to identify residues distal from the catalytic domain that contribute to enzyme activity and substrate selectivity. Amino acids roughly 50 Å (for the CTD1) and as far away as 60−70 Å (CTD2) were major contributors to catalysis. In particular, at least four residues in the HTH motif of the CTD2 are essential for catalysis (Figure 3A). At some positions, even conservative changes led to catalytic loss, for example N413Q, Q416N, and R425K. In the first helix of the HTH motif, introduction of lysine residues at T410 and N413 restored activity despite these positions not being positively charged in the wild-type BcTilS enzyme (Figure 3B). The robust lysidinylation activity could be attributed to enhanced electrostatic stabilization of the protein-tRNA complex. At least one of these positions is a lysine residue in EcTilS and GkTilS homologues, and the restored activity may represent a structural adaptability in acceptor stem recognition.

While Type I TilS enzymes clearly depend on nucleotides in the $tRNA^{Ile2}$ acceptor stem, recognition is more than direct and conserved readout of a single base pair, as is observed for example in the G3:U70 pair of $tRNA^{Ala}$ used by alanyl-tRNA synthetase enzymes in all domains of life.[49] Instead, a catalytically competent TilS:tRNA complex requires elements distributed across the enzyme. We propose that the HTH motif in CTD2 contains three residues on the face of Helix 1 that project into the major groove of the acceptor stem, providing direct readout of identity elements, and that the conserved R425 contributes electrostatic stabilization. Not surprisingly, truncation of the CTD2 reduced lysidinylation dramatically but not completely. At elevated concentration, the ΔCTD2 variant was able not only to lysidinylate its cognate $tRNA^{Ile2}$, but also use the noncognate C3:G70 variant (Figure 4).

Efficient lysidinylation of $tRNA^{Ile2}$ by Type I enzymes like BcTilS depends on readout of key acceptor stem nucleotides and either shape readout or direct recognition of other regions of the tRNA.[29] The need to reject near-cognate $tRNA^{Met}$ is likely the driving force for CTD2 contacts with the acceptor stem in Type I enzymes, but even CTD1 must retain some discrimination. This is evidenced in the inability of the ΔCTD2 variant to lysidinylate $tRNA^{Met}$, despite robustly acting on the C3:G70 $tRNA^{Ile2}$ variant (Figure 4).

The CTD1 proximal to the catalytic site also contributes to activity, although perhaps not through direct base readout. Alanine substitutions in the helix of the Helix-Turn-Sheet motif decrease activity more than those in the sheet portion, which is consistent with its closer approach to the tRNA anticodon stem. More of the CTD1 positions tested impacted enzyme function than those in CTD2, perhaps due to the proximity to the catalytic domain in general. The activity of the R301A variant is especially notable, as it lysidinylates $tRNA^{Ile2}$ at an initial rate approximately twice that of the wild-type TilS (Figure 5). Given its apparent position in the GkTilS:BstR-NA^{Ile2} complex, R301 may be a key "sensor" of the L-shaped tRNA.[53] We envision the guanidinium side-chain acting as a brake to limit productive conformational rearrangement of the protein:tRNA complex in the absence of distal identity elements. Increased activity for the R301A variant suggests that removing the guanidinium group more readily promotes a catalytically active conformation.

The observation that regions remote from the catalytic site impact activity suggests a signaling network between protein domains, likely driven by cognate tRNA binding. Indeed, comparing structures of apo-EcTilS with tRNA-bound GkTilS indicate a dramatic domain rotation of CTD2 upon tRNA binding.[29] The engineered double mutant T410K/R301A may capture some of the signaling network, as it is both more active than either single variant with respect to the cognate substrate and promotes robust lysidinylation of the C3:G70 $tRNA^{Ile2}$ variant (Figure 7).

Despite the apparent essentiality of TilS for translational accuracy, this family of enzymes exhibits diverse structural organization and subtle differences in substrate discrimination. Co-evolution between TilS and $tRNA^{Ile2}$ presumably influenced the need for acceptor stem recognition in some species but not others. It remains to be determined how Type II enzymes lacking CTD2 differentiate between the cognate $tRNA^{Ile2}$ and near-cognate $tRNA^{Met}$, and how Type I enzymes signal the presence of acceptor stem nucleotides up to 70 Å away from the catalytic site. Further mechanistic questions could be answered by structural studies of Type II enzymes in complex with cognate tRNA and computational analysis of the variants described here.

■ ASSOCIATED CONTENT

Supporting Information

The Supporting Information is available free of charge at https://pubs.acs.org/doi/10.1021/acsomega.5c00897.

Initial and relative lysidinylation rates of tRNA and enzyme variants (Tables S1−S5) (PDF)

Accession Codes

B. cenocepacia TilS: UniProt ID A0A3R9CE37

■ AUTHOR INFORMATION

Corresponding Author

Rebecca W. Alexander − *Department of Chemistry and Center for Molecular Signaling, Wake Forest University, Winston-Salem, North Carolina 27109, United States;* orcid.org/0000-0002-9159-6991; Email: alexanr@wfu.edu

Authors

Ferdiemar C. Guinto, Jr. − *Department of Chemistry and Center for Molecular Signaling, Wake Forest University,*

https://doi.org/10.1021/acsomega.5c00897
ACS Omega 2025, 10, 11618−11626

Winston-Salem, North Carolina 27109, United States; orcid.org/0009-0007-4278-2492

Samantha C. Robinson − *Department of Chemistry and Center for Molecular Signaling, Wake Forest University, Winston-Salem, North Carolina 27109, United States;* Present Address: University of California Davis, Davis, California 95616, USA

Complete contact information is available at: https://pubs.acs.org/10.1021/acsomega.5c00897

Author Contributions

The manuscript was written through contributions of all authors. F.C.G, Jr. and S.C.R. performed the experiments; R.W.A. and F.C.G., Jr. wrote the manuscript. All authors have given approval to the final version of the manuscript.

Funding

This work was supported by the National Science Foundation (MCB-1818131). F.C.G., Jr. was a recipient of a T32 graduate fellowship (GM095440) and a Center for Molecular Signaling Graduate Research Fellowship. S.C.R. was a recipient of a Center for Molecular Signaling Undergraduate Summer Fellowship.

Notes

The authors declare no competing financial interest.

■ ACKNOWLEDGMENTS

The authors thank Vaughn Cooper, Marc Muraski, and Emil Nilsson for helpful discussions on this project.

■ REFERENCES

(1) Lorenz, C.; Lünse, C. E.; Mörl, M. tRNA Modifications: Impact on Structure and Thermal Adaptation. *Biomolecules* **2017**, *7*, 35.

(2) Suzuki, T. The expanding world of tRNA modifications and their disease relevance. *Nat. Rev. Mol. Cell Biol.* **2021**, *22*, 375−392.

(3) Yared, M.-J.; Marcelot, A.; Barraud, P. Beyond the Anticodon: tRNA Core Modifications and Their Impact on Structure. *Translation and Stress Adaptation. Genes* **2024**, *15*, 374.

(4) Zhang, W.; Foo, M.; Eren, A. M.; Pan, T. tRNA modification dynamics from individual organisms to metaepitranscriptomics of microbiomes. *Mol. Cell* **2022**, *82*, 891−906.

(5) Schultz, S. K.; Kothe, U. RNA modifying enzymes shape tRNA biogenesis and function. *J. Biol. Chem.* **2024**, *300*, No. 107488.

(6) Agris, P. F.; Eruysal, E. R.; Narendran, A.; Väre, V. Y. P.; Vangaveti, S.; Ranganathan, S. V. Celebrating wobble decoding: Half a century and still much is new. *RNA Biology* **2018**, *15*, 537−553.

(7) Rafels-Ybern, À.; Torres, A. G.; Camacho, N.; Herencia-Ropero, A.; Roura Frigolé, H.; Wulff, T. F.; Raboteg, M.; Bordons, A.; Grau-Bove, X.; Ruiz-Trillo, I.; Ribas de Pouplana, L. The Expansion of Inosine at the Wobble Position of tRNAs, and Its Role in the Evolution of Proteomes. *Mol. Biol. Evol.* **2019**, *36*, 650−662.

(8) Krüger, M. K.; Pedersen, S.; Hagervall, T. G.; Sørensen, M. A. The modification of the wobble base of $tRNA^{Glu}$ modulates the translation rate of glutamic acid codons *in vivo*. *J. Mol. Biol.* **1998**, *284*, 621−631.

(9) Soma, A.; Ikeuchi, Y.; Kanemasa, S.; Kobayashi, K.; Ogasawara, N.; Ote, T.; Kato, J.; Watanabe, K.; Sekine, Y.; Suzuki, T. An RNA-Modifying Enzyme that Governs Both the Codon and Amino Acid Specificities of Isoleucine tRNA. *Mol. Cell* **2003**, *12*, 689−698.

(10) Grosjean, H.; Björk, G. R. Enzymatic conversion of cytidine to lysidine in anticodon of bacterial $tRNA^{Ile}$ − an alternative way of RNA editing. *Trends Biochem. Sci.* **2004**, *29*, 165−168.

(11) Ikeuchi, Y.; Soma, A.; Ote, T.; Kato, J.; Sekine, Y.; Suzuki, T. Molecular Mechanism of Lysidine Synthesis that Determines tRNA Identity and Codon Recognition. *Mol. Cell* **2005**, *19*, 235−246.

(12) Suzuki, T.; Miyauchi, K. Discovery and characterization of $tRNA^{Ile}$ lysidine synthetase (TilS). *FEBS Lett.* **2010**, *584*, 272−277.

(13) Muramatsu, T.; Yokoyama, S.; Horie, N.; Matsuda, A.; Ueda, T.; Yamaizumi, Z.; Kuchino, Y.; Nishimura, S.; Miyazawa, T. A novel lysine-substituted nucleoside in the first position of the anticodon of minor isoleucine tRNA from *Escherichia coli*. *J. Biol. Chem.* **1988**, *263*, 9261−9267.

(14) Bohlke, N.; Budisa, N. Sense codon emancipation for proteome-wide incorporation of noncanonical amino acids: rare isoleucine codon AUA as a target for genetic code expansion. *FEMS Microbiology Letters* **2014**, *351*, 133−144.

(15) Voorhees, R. M.; Mandal, D.; Neubauer, C.; Köhrer, C.; RajBhandary, U. L.; Ramakrishnan, V. The structural basis for specific decoding of AUA by isoleucine tRNA on the ribosome. *Nat. Struct Mol. Biol.* **2013**, *20*, 641−643.

(16) Akiyama, N.; Ishiguro, K.; Yokoyama, T.; Miyauchi, K.; Nagao, A.; Shirouzu, M.; Suzuki, T. Structural insights into the decoding capability of isoleucine tRNAs with lysidine and agmatidine. *Nat. Struct Mol. Biol.* **2024**, *31*, 817−825.

(17) Miyauchi, K.; Kimura, S.; Akiyama, N.; Inoue, K.; Ishiguro, K.; Vu, T.-S.; Srisuknimit, V.; Koyama, K.; Hayashi, G.; Soma, A.; Nagao, A.; Shirouzu, M.; Okamoto, A.; Waldor, M. K.; Suzuki, T. A tRNA modification with aminovaleramide facilitates AUA decoding in protein synthesis. *Nat. Chem. Biol.* **2024**, 1−10.

(18) Numata, T. Mechanisms of the tRNA wobble cytidine modification essential for AUA codon decoding in prokaryotes. *Biosci., Biotechnol., Biochem.* **2015**, *79*, 347−353.

(19) Suzuki, T.; Numata, T. Convergent evolution of AUA decoding in bacteria and archaea. *RNA Biology* **2014**, *11*, 1586−1596.

(20) Osawa, T.; Kimura, S.; Terasaka, N.; Inanaga, H.; Suzuki, T.; Numata, T. Structural basis of tRNA agmatinylation essential for AUA codon decoding. *Nat. Struct Mol. Biol.* **2011**, *18*, 1275−1280.

(21) Mandal, D.; Köhrer, C.; Su, D.; Russell, S. P.; Krivos, K.; Castleberry, C. M.; Blum, P.; Limbach, P. A.; Söll, D.; RajBhandary, U. L. Agmatidine, a modified cytidine in the anticodon of archaeal $tRNA^{Ile}$, base pairs with adenosine but not with guanosine. *Proc. Natl. Acad. Sci. U. S. A.* **2010**, *107*, 2872−2877.

(22) Dong, J.; Li, F.; Gao, F.; Wei, J.; Lin, Y.; Zhang, Y.; Lou, J.; Liu, G.; Dong, Y.; Liu, L.; Liu, H.; Wang, J.; Gong, W. Structure of tRNA-Modifying Enzyme TiaS and Motions of Its Substrate Binding Zinc Ribbon. *J. Mol. Biol.* **2018**, *430*, 4183−4194.

(23) Rybak, M. Y.; Gagnon, M. G. Structures of the ribosome bound to EF-Tu−isoleucine tRNA elucidate the mechanism of AUG avoidance. *Nat. Struct Mol. Biol.* **2024**, *31*, 810−816.

(24) Taniguchi, T.; Miyauchi, K.; Nakane, D.; Miyata, M.; Muto, A.; Nishimura, S.; Suzuki, T. Decoding system for the AUA codon by $tRNA^{Ile}$ with the UAU anticodon in *Mycoplasma mobile*. *Nucleic Acids Res.* **2013**, *41*, 2621−2631.

(25) Senger, B.; Auxilien, S.; Englisch, U.; Cramer, F.; Fasiolo, F. The Modified Wobble Base Inosine in Yeast $tRNA^{Ile}$ Is a Positive Determinant for Aminoacylation by Isoleucyl-tRNA Synthetase. *Biochemistry* **1997**, *36*, 8269−8275.

(26) Diwan, G. D.; Agashe, D. Wobbling Forth and Drifting Back: The Evolutionary History and Impact of Bacterial tRNA Modifications. *Mol. Biol. Evol.* **2018**, *35*, 2046−2059.

(27) Nakanishi, K.; Fukai, S.; Ikeuchi, Y.; Soma, A.; Sekine, Y.; Suzuki, T.; Nureki, O. Structural basis for lysidine formation by ATP pyrophosphatase accompanied by a lysine-specific loop and a tRNA-recognition domain. *Proc. Natl. Acad. Sci. U. S. A.* **2005**, *102*, 7487−7492.

(28) Kuratani, M.; Yoshikawa, Y.; Bessho, Y.; Higashijima, K.; Ishii, T.; Shibata, R.; Takahashi, S.; Yutani, K.; Yokoyama, S. Structural Basis of the Initial Binding of $tRNA^{Ile}$ Lysidine Synthetase TilS with ATP and L-Lysine. *Structure* **2007**, *15*, 1642−1653.

(29) Nakanishi, K.; Bonnefond, L.; Kimura, S.; Suzuki, T.; Ishitani, R.; Nureki, O. Structural basis for translational fidelity ensured by transfer RNA lysidine synthetase. *Nature* **2009**, *461*, 1144−8.

(30) Xie, W.; Liu, X.; Huang, R. H. Chemical trapping and crystal structure of a catalytic tRNA guanine transglycosylase covalent intermediate. *Nat. Struct Mol. Biol.* **2003**, *10*, 781−788.
(31) Losey, H. C.; Ruthenburg, A. J.; Verdine, G. L. Crystal structure of *Staphylococcus aureus* tRNA adenosine deaminase TadA in complex with RNA. *Nat. Struct Mol. Biol.* **2006**, *13*, 153−159.
(32) Muraski, M. J.; Nilsson, E. M.; Fritz, M. J.; Richardson, A. R.; Alexander, R. W.; Cooper, V. S. Adaptation to Overflow Metabolism by Mutations That Impair tRNA Modification in Experimentally Evolved Bacteria. *mBio* **2023**, *14*, No. e0028723.
(33) Liu, H.; Naismith, J. H. An efficient one-step site-directed deletion, insertion, single and multiple-site plasmid mutagenesis protocol. *BMC Biotechnology* **2008**, *8*, 91.
(34) Wang, W.; Malcolm, B. A. Two-Stage Polymerase Chain Reaction Protocol Allowing Introduction of Multiple Mutations, Deletions, and Insertions, Using QuikChangeTM Site-Directed Mutagenesis. In *In Vitro Mutagenesis Protocols*; (Braman, J., Ed.); Humana Press: Totowa, NJ, 2002, pp 37−43.
(35) Zheng, L.; Baumann, U.; Reymond, J.-L. An efficient one-step site-directed and site-saturation mutagenesis protocol. *Nucleic Acids Res.* **2004**, *32*, No. e115.
(36) Madeira, F.; Madhusoodanan, N.; Lee, J.; Eusebi, A.; Niewielska, A.; Tivey, A. R. N.; Lopez, R.; Butcher, S. The EMBL-EBI Job Dispatcher sequence analysis tools framework in 2024. *Nucleic Acids Res.* **2024**, *52*, W521−W525.
(37) Stothard, P. The Sequence Manipulation Suite: JavaScript Programs for Analyzing and Formatting Protein and DNA Sequences. *BioTechniques* **2000**, *28*, 1102−1104.
(38) Sherlin, L. D.; Bullock, T. L.; Nissan, T. A.; Perona, J. J.; Lariviere, F. J.; Uhlenbeck, O. C.; Scaringe, S. A. Chemical and enzymatic synthesis of tRNAs for high-throughput crystallization. *RNA* **2001**, *7*, 1671−1678.
(39) Chan, P. P.; Lowe, T. M. GtRNAdb: a database of transfer RNA genes detected in genomic sequence. *Nucleic Acids Res.* **2009**, *37*, D93−D97.
(40) Chan, P. P.; Lowe, T. M. GtRNAdb 2.0: an expanded database of transfer RNA genes identified in complete and draft genomes. *Nucleic Acids Res.* **2016**, *44*, D184−D189.
(41) Gil, R.; Silva, F. J.; Peretó, J.; Moya, A. Determination of the Core of a Minimal Bacterial Gene Set. *Microbiology and Molecular Biology Reviews* **2004**, *68*, 518−537.
(42) Grosjean, H.; Breton, M.; Sirand-Pugnet, P.; Tardy, F.; Thiaucourt, F.; Citti, C.; Barré, A.; Yoshizawa, S.; Fourmy, D.; de Crécy-Lagard, V.; Blanchard, A. Predicting the Minimal Translation Apparatus: Lessons from the Reductive Evolution of Mollicutes. *PLOS Genetics* **2014**, *10*, No. e1004363.
(43) Nilsson, E. M.; Alexander, R. W. Bacterial wobble modifications of NNA-decoding tRNAs. *IUBMB Life* **2019**, *71*, 1158−1166.
(44) Baba, T.; Ara, T.; Hasegawa, M.; Takai, Y.; Okumura, Y.; Baba, M.; Datsenko, K. A.; Tomita, M.; Wanner, B. L.; Mori, H. Construction of *Escherichia coli* K-12 in-frame, single-gene knockout mutants: the Keio collection. *Mol. Syst. Biol.* **2006**, *2*, 2006.
(45) Fabret, C.; Dervyn, E.; Dalmais, B.; Guillot, A.; Marck, C.; Grosjean, H.; Noirot, P. Life without the essential bacterial $tRNA^{Ile2}$-lysidine synthetase TilS: a case of tRNA gene recruitment in *Bacillus subtilis*. *Mol. Microbiol.* **2011**, *80*, 1062−1074.
(46) Kobayashi, K.; Ehrlich, S. D.; Albertini, A.; Amati, G.; Andersen, K. K.; Arnaud, M.; Asai, K.; Ashikaga, S.; Aymerich, S.; Bessieres, P.; Boland, F.; Brignell, S. C.; Bron, S.; Bunai, K.; Chapuis, J.; Christiansen, L. C.; Danchin, A.; Débarbouillé, M.; Dervyn, E.; Deuerling, E.; Devine, K.; Devine, S. K.; Dreesen, O.; Errington, J.; Fillinger, S.; Foster, S. J.; Fujita, Y.; Galizzi, A.; Gardan, R.; Eschevins, C.; Fukushima, T.; Haga, K.; Harwood, C. R.; Hecker, M.; Hosoya, D.; Hullo, M. F.; Kakeshita, H.; Karamata, D.; Kasahara, Y.; Kawamura, F.; Koga, K.; Koski, P.; Kuwana, R.; Imamura, D.; Ishimaru, M.; Ishikawa, S.; Ishio, I.; Le Coq, D.; Masson, A.; Mauël, C.; Meima, R.; Mellado, R. P.; Moir, A.; Moriya, S.; Nagakawa, E.; Nanamiya, H.; Nakai, S.; Nygaard, P.; Ogura, M.; Ohanan, T.; O'Reilly, M.; O'Rourke, M.; Pragai, Z.; Pooley, H. M.; Rapoport, G.; Rawlins, J. P.; Rivas, L. A.; Rivolta, C.; Sadaie, A.; Sadaie, Y.; Sarvas, M.; Sato, T.; Saxild, H. H.; Scanlan, E.; Schumann, W.; Seegers, J. F. M. L.; Sekiguchi, J.; Sekowska, A.; Séror, S. J.; Simon, M.; Stragier, P.; Studer, R.; Takamatsu, H.; Tanaka, T.; Takeuchi, M.; Thomaides, H. B.; Vagner, V.; van Dijl, J. M.; Watabe, K.; Wipat, A.; Yamamoto, H.; Yamamoto, M.; Yamamoto, Y.; Yamane, K.; Yata, K.; Yoshida, K.; Yoshikawa, H.; Zuber, U.; Ogasawara, N. Essential Bacillus subtilis genes. *Proc. Natl. Acad. Sci. U. S. A.* **2003**, *100*, 4678−4683.
(47) Ghomi, F. A.; Jung, J. J.; Langridge, G. C.; Cain, A. K.; Boinett, C. J.; Abd El Ghany, M.; Pickard, D. J.; Kingsley, R. A.; Thomson, N. R.; Parkhill, J.; Gardner, P. P.; Barquist, L. High-throughput transposon mutagenesis in the family Enterobacteriaceae reveals core essential genes and rapid turnover of essentiality. *mBio* **2024**, *15*, No. e0179824.
(48) Giegé, R.; Eriani, G. The tRNA identity landscape for aminoacylation and beyond. *Nucleic Acids Res.* **2023**, *51*, 1528−1570.
(49) Chong, Y. E.; Guo, M.; Yang, X.-L.; Kuhle, B.; Naganuma, M.; Sekine, S.; Yokoyama, S.; Schimmel, P. Distinct ways of G:U recognition by conserved tRNA binding motifs. *Proc. Natl. Acad. Sci. U. S. A.* **2018**, *115*, 7527−7532.
(50) Ben Chorin, A.; Masrati, G.; Kessel, A.; Narunsky, A.; Sprinzak, J.; Lahav, S.; Ashkenazy, H.; Ben-Tal, N. ConSurf-DB: An accessible repository for the evolutionary conservation patterns of the majority of PDB proteins. *Protein Sci.* **2020**, *29*, 258−267.
(51) Lin, T.-H.; Hu, Y.-N.; Shaw, G.-C. Two enzymes, TilS and HprT, can form a complex to function as a transcriptional activator for the cell division protease gene ftsH in *Bacillus subtilis*. *Journal of Biochemistry* **2014**, *155*, 5−16.
(52) Thiaville, P. C.; El Yacoubi, B.; Köhrer, C.; Thiaville, J. J.; Deutsch, C.; Iwata-Reuyl, D.; Bacusmo, J. M.; Armengaud, J.; Bessho, Y.; Wetzel, C.; Cao, X.; Limbach, P. A.; RajBhandary, U. L.; de Crécy-Lagard, V. Essentiality of threonylcarbamoyladenosine (t6A), a universal tRNA modification, in bacteria. *Mol. Microbiol.* **2015**, *98*, 1199.
(53) McKenney, K. M.; Rubio, M. A. T.; Alfonzo, J. D. The Evolution of Substrate Specificity by tRNA Modification Enzymes. *Enzymes* **2017**, *41*, 51−88.

https://doi.org/10.1021/acsomega.5c00897
ACS Omega 2025, 10, 11618−11626